Published in final edited form as:
Angew Chem Int Ed Engl. 2012 March 12; 51(11): 2731–2735. doi:10.1002/anie.201108132.

Dual Acquisition Magic Angle Spinning (DUMAS) Solid-State NMR: A New Approach to Simultaneous Acquisition of Multidimensional Spectra of Biomacromolecules

T. Gopinath and **Gianluigi Veglia***
Department of Chemistry and Department of Biochemistry, Molecular Biology and Biophysics, 321 Church St. SE, Minneapolis, MN 55455 USA

Keywords

Dual Acquisition; Magic Angle Spinning; Solid-State NMR; Proteins; Simultaneous Cross-Polarization; Long Living ^{15}N Polarization

Magic angle spinning solid-state NMR (MAS ssNMR) spectroscopy is a powerful method for atomic-resolution structure determination of biomacromolecules that are recalcitrant to crystallization (membrane proteins and fibrils).[1, 2, 2–4] Developments in pulse sequence design,[5–10] probes,[11] isotopic-labeling schemes,[12], sensitivity enhancement using paramagnetic effects [13], dynamic nuclear polarization (DNP)[14–16], and sample preparations have made it possible to advance resonance assignments and structure determination by ssNMR. However, as the biological systems under investigation increase in complexity, new methods are needed to improve spectral resolution and sensitivity as well as speed up NMR data acquisition.

Here we present a novel approach (which we refer as “dual acquisition MAS ssNMR or DUMAS ssNMR) for parallel acquisition of multidimensional ssNMR experiments without the need of additional hardware. DUMAS ssNMR is able to combine several of the above advancements to almost double the capability of the NMR spectrometers. Central to this technique are the following phenomena: 1) the long-living ^{15}N polarization in biological solids; 2) Simultaneous Hartmann-Hahn (HH) cross polarization (CP) from ^{1}H to ^{13}C and ^{15}N, and 3) ^{15}N-^{13}C dipolar decoupling under MAS conditions. DUMAS is not limited to specific pulse sequences, rather it represents a general approach to concatenate various multidimensional ssNMR experiments.

The classical ssNMR experiments start with HH-CP,[17, 18], which enhances the sensitivity of rare nuclei coupled to abundant ^{1}H spin bath. However, during CP only part of the polarization from ^{1}H spin bath is transferred to dilute spins (^{13}C or ^{15}N). Recently, Oschkinat and co-workers proposed to enhance ^{13}C sensitivity with triple resonance (^{1}H, ^{2}H, ^{13}C) CP using perdeuterated proteins.[19] Analogously, for DUMAS we utilize simultaneous CP (SIM-CP) to polarize ^{13}C and ^{15}N. We then exploit the polarization to acquire two ^{13}C- and ^{15}N-edited multidimensional experiments in parallel. Since the ^{15}N nuclei have relatively long longitudinal spin relaxation times (T_1),[20] the ^{15}N z-magnetization can be stored for several milliseconds (while acquiring ^{13}C coherences) and recovered for an additional multidimensional experiment.

*vegli001@umn.edu, Homepage: www.chem.umn.edu/groups/veglia.

Supporting information for this article is available on the WWW under http://www.angewandte.org

A schematic of DUMAS is reported in Figure 1A. A 90° pulse on ^{1}H is followed by SIM-CP and creates the initial polarization of ^{13}C and ^{15}N nuclei. After SIM-CP, the ^{15}N magnetization is tilted along the z-axis by a 90° pulse, whereas the ^{13}C magnetization is used to record a ^{13}C-edited spectrum with t_1' indirect evolution and t_2' acquisition under two-pulse phase modulated (TPPM) heteronuclear decoupling.[21]

After the acquisition of the first experiment, a τ delay of 2 ms is used to dephase any residual magnetization. Namely, in the first $\tau/2$ period, the transverse magnetization is dephased, while the longitudinal magnetization is dephased by a 90° pulse, followed by another $\tau/2$ period. A delay $T = [t_{1max}' - dw(t_1')]$ is applied under heteronuclear decoupling, where t_{1max}' is the maximum t_1', and $dw(t_1')$ is dwell time of the t_1' evolution period. This delay makes the total time of the ^{13}C-edited acquisition identical for all of the t_1' increments, while the ^{15}N magnetization is stored along the z-axis. A $90_y°$ pulse recovers the ^{15}N magnetization stored along the z-axis and places it along the x-axis. At this point, a ^{15}N-edited sequence block is implemented followed by a second acquisition on ^{13}C channel during t_2". Due to the different relaxation behaviors, the evolution times (t_1) are usually longer for ^{15}N than ^{13}C. Our scheme uses separate evolution time periods (t_1' and t_1"), which can be optimized for both sensitivity and resolution according to Table S1. Although it is possible to combine various multidimensional experiments, we demonstrate the DUMAS method concatenating DARR,[22], NCA,[23] DQSQ,[24], and NCO,[23] four of the most widely used pulse sequences for structure determination of proteins. Specifically, we incorporated the ^{13}C- and ^{15}N-edited blocks to create the DUMAS-DARR-NCA and DUMAS-DQSQ-NCO pulse sequences (Figure 1).

To test the performance of these experiments, we used uniformly (U)-^{13}C, ^{15}N ubiquitin in microcrystalline form, which is the benchmark for MAS ssNMR experiments on proteins.[25] U-^{13}C, ^{15}N labeled ubiquitin powder sample (10 mg) was dissolved in citrate buffer (20 mM, pH 4.1) to obtain a solution of 35 mg/mL. The protein was then crystallized by adding 2-methyl-2,4-pentanediol (60% final volume).[25, 26] Approximately, 5mg of microcrystalline ubiquitin was loaded into the MAS rotor. We also demonstrate that DUMAS pulse sequences can be applied to more challenging systems such as integral membrane protein phospholamban reconstituted in lipid membrane. Phospholamban (52 residues)[27–29] was expressed recombinantly in *E. coli*[30] and reconstituted in lipid membranes as previously reported[31].

For the DARR, DQSQ, NCA and NCO pulse sequences (Figures 1S, panels A–C), the initial ^{1}H-^{13}C or ^{1}H-^{15}N CP was optimized using the conventional CP experiment shown in Figure 1S. During SIM-CP, ^{1}H-^{13}C, or ^{1}H-^{15}N CP, the radio frequency (RF) field strengths of ^{1}H, ^{13}C and ^{15}N were 45, 36.7, and 36.7 kHz, respectively, which corresponds to n=1 side band matching condition. The ^{1}H RF amplitude was ramped by 10% with center of the slope equal to 45 kHz. For comparison, the spectra obtained with $^{1}H/^{13}C$ CP and ^{13}C-detected $^{1}H/^{13}C/^{15}N$ SIM-CP at various contact times are reported in Figure 2S. Notably, the sensitivity in the ^{13}C spectral region between 0 and 80 ppm is nearly identical for both CP and SIM-CP at all contact times. The ^{13}C sensitivity in the carbonyl region of ^{13}C spectrum (Figure 3S) is 5–15 % higher for the spectrum acquired with CP. However, the carbonyl region of ^{13}C-^{13}C correlation spectra is often neglected due to inherent low sensitivity and resolution. The comparison of $^{1}H/^{15}N$ CP and ^{15}N detected $^{1}H/^{13}C/^{15}N$ SIM-CP spectra at various contact times (Figure 4S) shows a sensitivity loss of ~12–23 % for SIM-CP. The integrated peak intensities from the spectra (Figures 2S and 4S) as function of the contact time are plotted in Figure 5S. Note that we have also tested CP and SIM-CP experiments on U-^{13}C,^{15}N N-acetyl Valine-Leucine dipeptide powder. Indeed, we obtained relative sensitivities similar to those obtained for microcrystalline ubiquitin and phospholamban in lipids. Although it is difficult to derive a theoretical (quantitative)

expression for SIM-CP, it should be noted that the rate of ^{13}C and ^{15}N polarization enhancement versus contact time is similar for both CP and SIM-CP experiments (Figures 5S). The latter indicates that the spin dynamics for CP and SIM-CP are qualitatively similar. Since only a moderate loss of sensitivity is observed for ^{15}N spectra (10–23%), we deduce that more polarization from the ^{1}H bath to the heteronuclei is transferred during SIM-CP compared to double resonance CP (^{1}H-^{13}C or ^{1}H-^{15}N). In fact Pines and co-workers [17] showed that more ^{1}H polarization can be transferred using multiple contact periods of ^{1}H-^{13}C CP. For SIM-CP, the ^{13}C and ^{15}N spin lock periods do not have to be identical. For example longer ^{13}C (or ^{15}N) spin lock period can be used in SIM-CP to improve the sensitivity of dynamic regions of the biopolymers or for side chain detection. For the ubiquitin sample, we found that contact times of 400 and 600 μs give optimum sensitivity for ^{1}H-^{13}C and ^{1}H-^{15}N CP, respectively (Figures 2S and 4S); whereas 400 μs was optimal for SIM-CP. For PLN, we used CP contact times of 300 and 500 μs for ^{1}H-^{13}C and ^{1}H-^{15}N CP respectively, whereas 300 μs for SIM-CP. With the exception of the contact time, all of the other experimental parameters used for DUMAS were identical to the conventional pulse sequences. Moreover, we tested the decay of ^{15}N magnetization stored along the z-axis after SIM-CP. Indeed, we found that the magnetization decay is negligible during the first ^{13}C-edited acquisition (Figure 6S).

Figure 2A shows the NCA and DARR spectra recorded using conventional 2D pulse sequences (Figure 1S). The total experimental time for both spectra was 16.03 hours. Figure 2B shows the corresponding spectra recorded simultaneously using the DUMAS-DARR-NCA experiment. The total experimental time was 8.12 hours. As expected, the sensitivity of DUMAS-DARR is identical to the conventional DARR, whereas the sensitivity of DUMAS-NCA is about 80% of the NCA spectrum, which is due to the implementation of the SIM-CP. A similar situation is presented for the NCO and DQSQ spectra. Figure 3A shows the two spectra acquired with the conventional methods for a total acquisition time of 15.57 hours. Figure 3B shows the corresponding spectra acquired simultaneously with DUMAS-DQSQ-NCO with a total experimental time of 8.06 hours, which is roughly ½ the time spent with conventional methods. As for the NCA, the sensitivity loss for the DUMAS-NCO is approximately 20%, while the DUMAS-DQSQ spectrum is similar to the conventional DQSQ. Figure 4 shows the application of DUMAS on U-^{13}C,^{15}N labeled membrane protein phospholamban. Each of the conventional spectra DARR and NCA were recorded in ~16 hours, while DUMAS spectra were acquired simultaneously in ~16 hours. These results demonstrate that the DUMAS is extendable to integral membrane proteins as well.

Note that for the DUMAS experiments, the parameters for the indirect acquisition of ^{13}C and ^{15}N are such that $ni(t_1')\bullet nt(t_1') = ni(t_1'')\bullet nt(t_1'')$ according to Table S1. In general, the optimum number of scans and increments (total number of 1D experiments) depend on the nature of ^{13}C- and ^{15}N-edited experiments. Since the ^{13}C- and ^{15}N- edited blocks are in different time periods, DUMAS gives the flexibility to acquire an insensitive ^{13}C-edited experiment using a greater number of scans, and multiple (two or more) ^{15}N-edited 2D experiments, or vice versa. In other words, a longer ^{13}C-edited experiment can be combined with multiple ^{15}N edited experiments, or vice versa.

In the past years, there has been a consistent effort to *make the best out of polarization* for both solution and solid-state NMR experiments[32–35]. An approach involves the recovery of discarded coherences to acquire an additional experiment[36–38] or obtain sensitivity enhancement of the NMR signals.[39–43] Another example is the simultaneous acquisition of ^{13}C- and ^{15}N-edited experiments in liquid-state NMR using single acquisition on the ^{1}H channel[44]. In the latter experiment, the evolution of ^{13}C and ^{15}N nuclear spins is coupled to ^{1}H spins through two-spin operators, limiting its performance. In ssNMR

spectroscopy, ^{15}N nuclei have long T_1 relaxation values in the order of few hundred milliseconds. For the first time, we utilized this unique property in combination with a SIM-CP scheme to exploit an untapped source of polarization and generate multiple experiments simultaneously. More importantly, DUMAS can be applied in combination with several sensitivity and resolution enhancement methods. For instance, it can benefit from protein perdeuteration[45]. To this extent, it has been shown that the values of ^{15}N T_1 for perdeuterated protein samples are not significantly different from the protonated ones[46]. A recent paper by Oschkinat and co-workers[47] shows that triple CP ^{1}H/^{2}H/^{13}C is substantially more sensitive than conventional ^{1}H/^{13}C CP. Based on this work, we can anticipate that quadruple ^{1}H/^{2}H/^{13}C/^{15}N CP using four channel probe with DUMAS acquisition will further enhance the sensitivity of these experiments.

DUMAS can also be used in concert with paramagnetic relaxation enhancements methods[13], obtaining faster data acquisition. In fact, it has been shown that for PRE samples the loss of ^{15}N z-magnetization in the absence of ^{1}H decoupling is less than ~10 % for 100 ms[48]. Therefore, DUMAS can also be successfully applied in combination with PRE enhancement [49, 50].

Another recent improvement for sensitivity enhancement of ssNMR is the implementation of DNP[14–16, 51]. This technique boosts the signal-to-noise ratio (S/N) of NMR spectra taking advantage of the polarization transfer of electronic spins to nuclear spins, doping the samples with nitroxide spin labels. If DNP is applicable to the sample under analysis, DUMAS can be coupled with methods to further speed up data acquisition and push the sensitivity limits of MAS ssNMR.

In conclusion, we introduce a novel approach for the simultaneous acquisition of ^{13}C- and ^{15}N-edited multidimensional MAS ssNMR experiments without additional hardware. Multidimensional DUMAS experiments are demonstrated on microcrystalline ubiquitin as well as PLN in lipid vesicles. The DUMAS scheme opens up new avenues for reducing the acquisition time for multi-dimensional experiments for biomolecular ssNMR by combining the sensitivity and resolution advancements obtained in the past few years. We anticipate that the combination of DUMAS with dynamic nuclear polarization[15, 16, 51], proton detection[8, 52], PRE and multiple receivers,[53] will further increase sensitivity, resolution as well as the number of experiments that can be acquired simultaneously.

Experimental Section

All of the NMR experiments were performed using a 700 MHz VNMRS spectrometer (Agilent Technologies). The spectrometer wasequipped with a 3.2 mm bioMAS scroll coil probe with reduced RF heating. [11] A spinning rate (ω_r) of 8.333 kHz was used for all of the experiments. Temperature was held constant at 5 °C. Further details on data acquisition are provided in the Supporting Information.

Supplementary Material

Refer to Web version on PubMed Central for supplementary material.

Acknowledgments

This work was supported by the National Institutes of Health (GM64742 and GM072701). We acknowledge M. Gustavsson, K. Mote, and F. Chao for preparing the samples and Dave Rice (Agilent) for helpful discussions.

References

1. McDermott A. Annu. Rev. Biophys. 2009; 38:385–403. [PubMed: 19245337]
2. Renault M, Cukkemane A, Baldus M. Angew. Chem. Int. Ed Engl. 2010; 49:8346–8357. [PubMed: 20941715]
3. Renault M, Bos MP, Tommassen J, Baldus M. J. Am. Chem. Soc. 2011; 133:4175–4177. [PubMed: 21361323]
4. Tycko R. Annu. Rev. Phys. Chem. 2011; 62:279–299. [PubMed: 21219138]
5. Baldus M. Progr NMR Spectr. 2002; 41:1–47.
6. Griffin RG. Nat. Struct. Biol. 1998; 5(Suppl):508–512. [PubMed: 9665180]
7. Wylie BJ, Rienstra CM. J. Chem. Phys. 2008; 128 052207.
8. Linser R, Dasari M, Hiller M, Higman V, Fink U, Lopez Del Amo JM, Markovic S, Handel L, Kessler B, Schmieder P, Oesterhelt D, Oschkinat H, Reif B. Angew. Chem. Int. Ed Engl. 2011; 50:4508–4512. [PubMed: 21495136]
9. Schuetz A, Wasmer C, Habenstein B, Verel R, Greenwald J, Riek R, Bockmann A, Meier BH. Chembiochem. 2010; 11:1543–1551. [PubMed: 20572250]
10. Franks WT, Kloepper KD, Wylie BJ, Rienstra CM. J. Biomol. NMR. 2007; 39:107–131. [PubMed: 17687624]
11. Stringer JA, Bronnimann CE, Mullen CG, Zhou DH, Stellfox SA, Li Y, Williams EH, Rienstra CM. J. Magn. Reson. 2005; 173:40–48. [PubMed: 15705511]
12. Lian L, Middleton DA. Progr NMR Spectr. 2001; 39:171–190.
13. Wickramasinghe NP, Parthasarathy S, Jones CR, Bhardwaj C, Long F, Kotecha M, Mehboob S, Fung LW, Past J, Samoson A, Ishii Y. Nat. Methods. 2009; 6:215–218. [PubMed: 19198596]
14. Maly T, Debelouchina GT, Bajaj VS, Hu KN, Joo CG, Mak-Jurkauskas ML, Sirigiri JR, van der Wel PC, Herzfeld J, Temkin RJ, Griffin RG. J. Chem. Phys. 2008; 128 052211.
15. Matsuki Y, Maly T, Ouari O, Karoui H, Le Moigne F, Rizzato E, Lyubenova S, Herzfeld J, Prisner T, Tordo P, Griffin RG. Angew. Chem. Int. Ed Engl. 2009; 48:4996–5000. [PubMed: 19492374]
16. Akbey U, Franks WT, Linden A, Lange S, Griffin RG, van Rossum BJ, Oschkinat H. Angew. Chem. Int. Ed Engl. 2010; 49:7803–7806. [PubMed: 20726023]
17. Pines A, Gibby MG, Waugh JS. Journal of Chemical Physics. 1973; 59:569–590.
18. Hartmann SR, Hahn EL. Phys. Rev. 1962; 128:2042.
19. Akbey U, Camponeschi F, van Rossum BJ, Oschkinat H. Chemphyschem. 2011
20. Giraud N, Bockmann A, Lesage A, Penin F, Blackledge M, Emsley L. J. Am. Chem. Soc. 2004; 126:11422–11423. [PubMed: 15366872]
21. Bennett AE, Rienstra CM, Auger M, Lakshmi KV, Griffin RG. J Chem Phys. 1995; 103:6951–6958.
22. Takegoshi K, Nakamura S, Terao T. Chem. Phys. Lett. 2001; 344:631.
23. Baldus M, Petkova AT, Herzfeld JH, Griffin RG. Mol. Phys. 1998; 95:1197–1207.
24. Hohwy M, Rienstra CM, Jaroniec CP, Griffin RG. J Chem Phys. 1999; 110:7983–7992.
25. Zech SG, Wand AJ, McDermott AE. J. Am. Chem. Soc. 2005; 127:8618–8626. [PubMed: 15954766]
26. Igumenova TI, McDermott AE, Zilm KW, Martin RW, Paulson EK, Wand AJ. J. Am. Chem. Soc. 2004; 126:6720–6727. [PubMed: 15161300]
27. Traaseth NJ, Ha KN, Verardi R, Shi L, Buffy JJ, Masterson LR, Veglia G. Biochemistry. 2008; 47:3–13. [PubMed: 18081313]
28. Traaseth NJ, Shi L, Verardi R, Mullen DG, Barany G, Veglia G. Proc. Natl. Acad. Sci. U. S. A. 2009; 106:10165–10170. [PubMed: 19509339]
29. Verardi R, Shi L, Traaseth NJ, Walsh N, Veglia G. Proc Natl Acad Sci U S A. 2011; 108:9101–9106. [PubMed: 21576492]
30. Buck B, Zamoon J, Kirby TL, DeSilva TM, Karim C, Thomas D, Veglia G. Protein Expr Purif. 2003; 30:253–261. [PubMed: 12880775]
31. Gustavsson M, Traaseth NT, Veglia G. BBA. 2011

32. Freeman R, Kupce E. Top. Curr. Chem. 2011
33. Kupce R, Freeman E. J. Magn. Reson. 2003; 163:56–63. [PubMed: 12852907]
34. Frydman L, Lupulescu A, Scherf T. J. Am. Chem. Soc. 2003; 125:9204–9217. [PubMed: 15369377]
35. Atreya HS, Szyperski T. Proc. Natl. Acad. Sci. U. S. A. 2004; 101:9642–9647. [PubMed: 15210958]
36. Fukuchi M, Takegoshi K. Solid State Nucl. Magn. Reson. 2008; 34:151–153. [PubMed: 18635343]
37. Kupce E, Kay LE, Freeman R. J. Am. Chem. Soc. 2010; 132:18008–18011. [PubMed: 21126087]
38. Gopinath T, Mote K, Veglia G. 2011 *(Under Review)*.
39. Kay LE, Keifer E, Saarinen T. J. Am. Chem. Soc. 1992; 114:10663–10665.
40. Tycko R. Chemphyschem. 2004; 5:863–868. [PubMed: 15253312]
41. Gopinath T, Veglia G. J. Am. Chem. Soc. 2009; 131:5754–5756. [PubMed: 19351170]
42. Gopinath T, Verardi R, Traaseth NJ, Veglia G. J Phys Chem B. 2010; 114:5089–5095. [PubMed: 20349983]
43. Gopinath T, Traaseth NJ, Mote K, Veglia G. J Am Chem Soc. 2010; 132:5357–5763. [PubMed: 20345172]
44. Pascal SM, Muhandiram DR, Yamazaki T, Forman-Kay JD, Kay LE. J Magn Reson. 2004; 103:197–201.
45. Crespi HL, Katz JJ. Methods Enzymol. 1972; 26 PtC:627–637. [PubMed: 4376580]
46. Chevelkov V, Diehl A, Reif B. J. Chem. Phys. 2008; 128 052316.
47. Akbey U, Camponeschi F, van Rossum BJ, Oschkinat H. Chemphyschem. 2011
48. Nadaud PS, Helmus JJ, Sengupta I, Jaroniec CP. J. Am. Chem. Soc. 2010; 132:9561–9563. [PubMed: 20583834]
49. Nadaud PS, Helmus JJ, Hofer N, Jaroniec CP. J. Am. Chem. Soc. 2007; 129:7502–7503. [PubMed: 17530852]
50. Nadaud PS, Helmus JJ, Kall SL, Jaroniec CP. J. Am. Chem. Soc. 2009; 131:8108–8120. [PubMed: 19445506]
51. Matsuki Y, Eddy MT, Griffin RG, Herzfeld J. Angew. Chem. Int. Ed Engl. 2010; 49:9215–9218. [PubMed: 20957710]
52. Huber M, Hiller S, Schanda P, Ernst M, Bockmann A, Verel R, Meier BH. Chemphyschem. 2011; 12:915–918. [PubMed: 21442705]
53. Kupce E, Freeman R, John BK. J. Am. Chem. Soc. 2006; 128:9606–9607. [PubMed: 16866495]

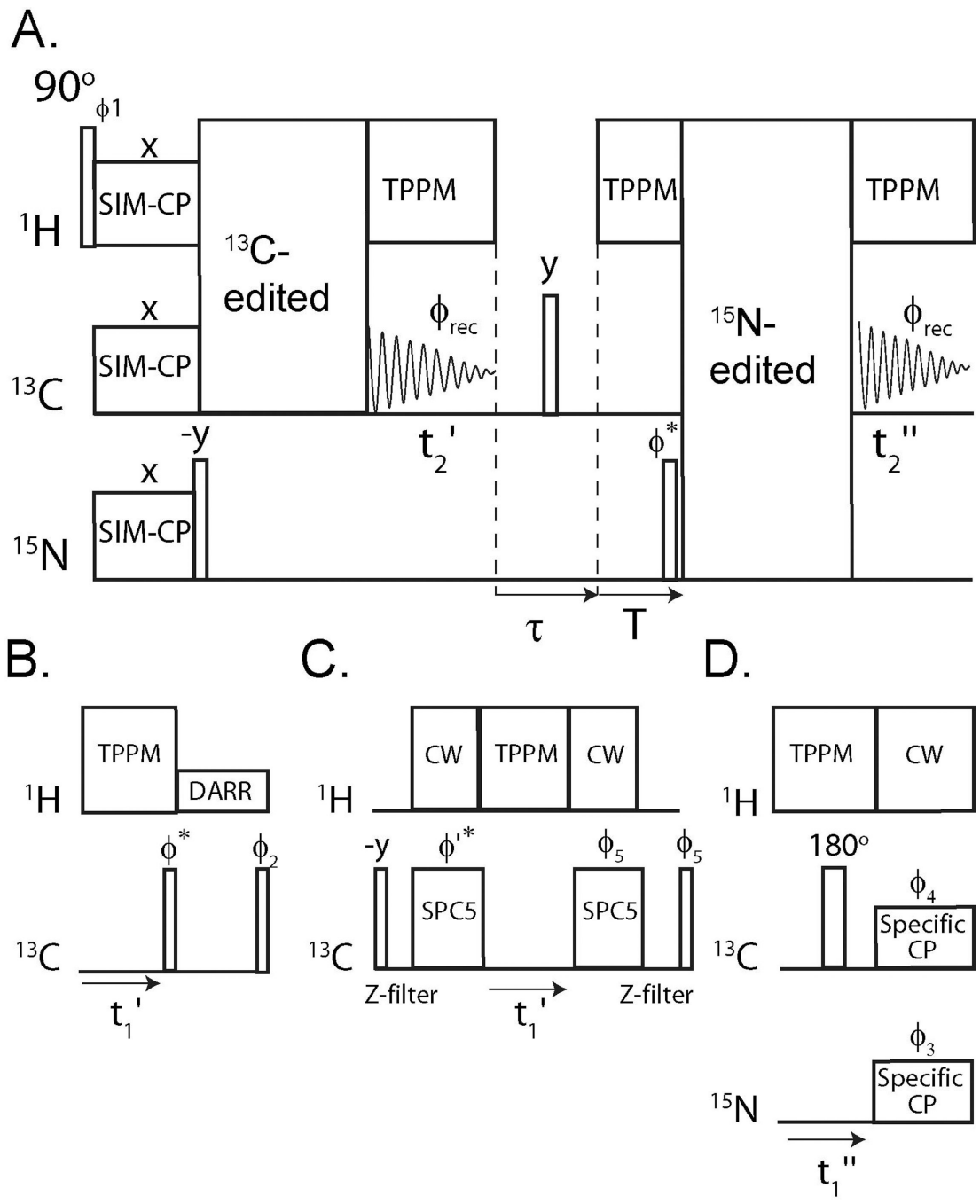

Figure 1.

(A) General scheme for the DUMAS ssNMR. The ^{13}C- and ^{15}N-edited blocks are combined to give DUMAS-DARR-NCA (B and D blocks) or DUMAS-DQSQ-NCO (C and D blocks).

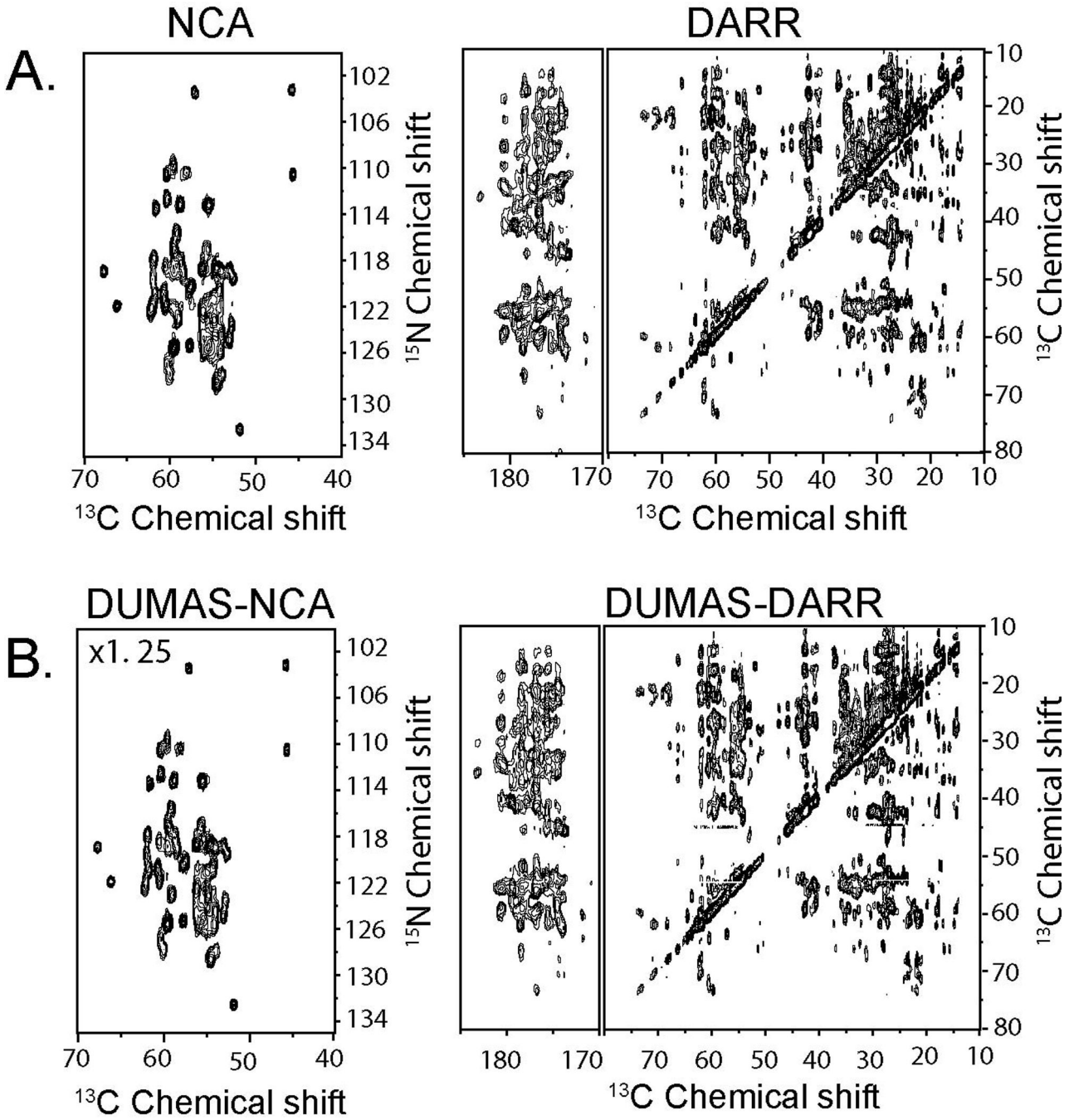

Figure 2.

(A) 2D NCA and DARR spectra of U-^{13}C,^{15}N-labeled ubiquitin acquired using conventional methods (Figure 1S). (B) NCA and DARR spectra acquired simultaneously using DUMAS-DARR-NCA pulse scheme. DARR and DUMAS-DARR are plotted with the identical noise level. DUMAS-NCA is plotted at 1.25 times the signal intensity of NCA to account for 20% signal loss of ^{15}N during SIM-CP.

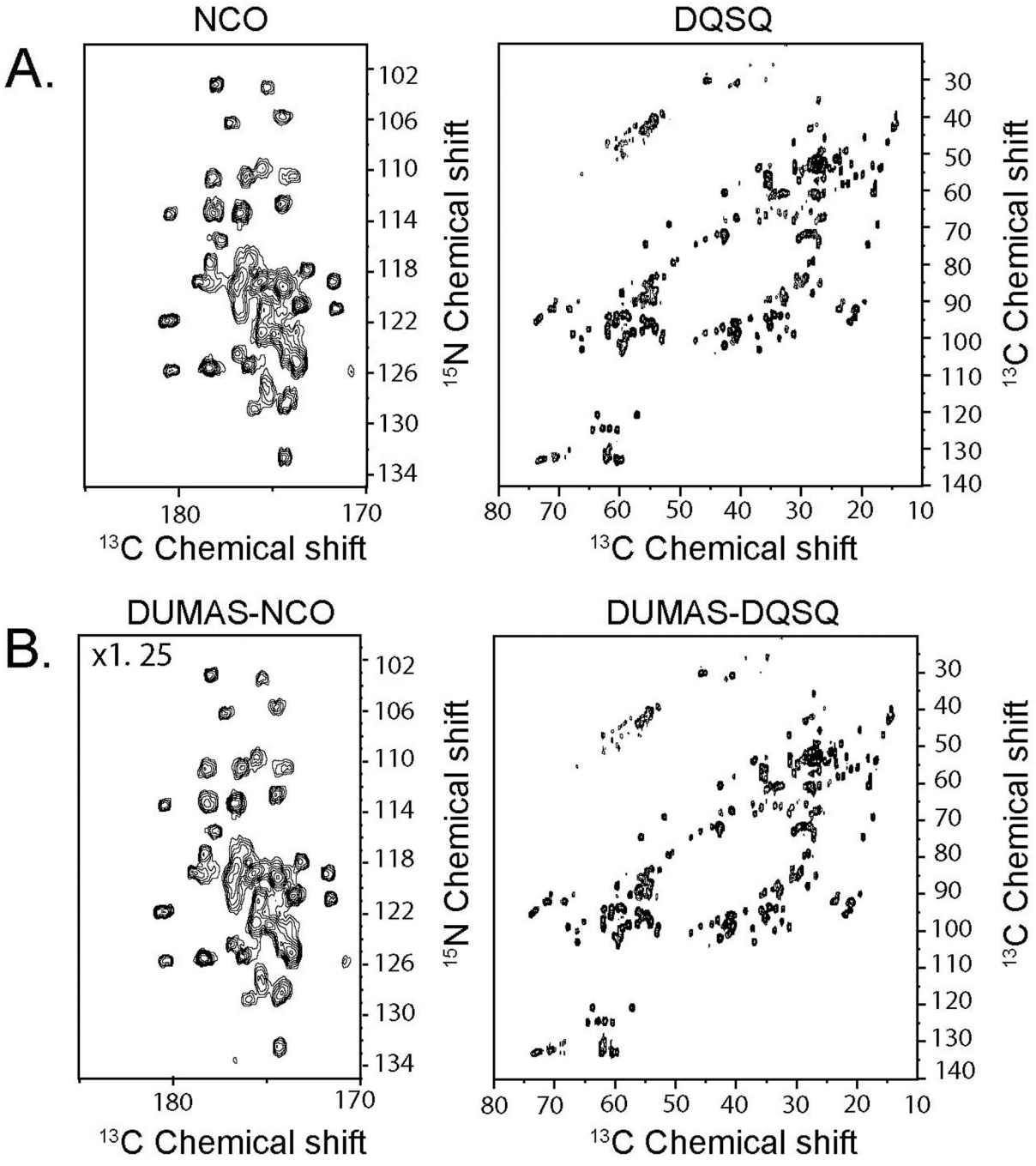

Figure 3.

(A) 2D NCO and DQSQ spectra acquired using conventional methods (Figure 1S). (B) NCO and DQSQ spectra acquired simultaneously using DUMAS-DQSQ-NCO. DQSQ and DUMAS-DQSQ are drawn at the same noise level. To account for 20 % signal loss of ^{15}N during SIM-CP, DUMAS-NCO is plotted with 1.25 times higher scale compared to NCO.

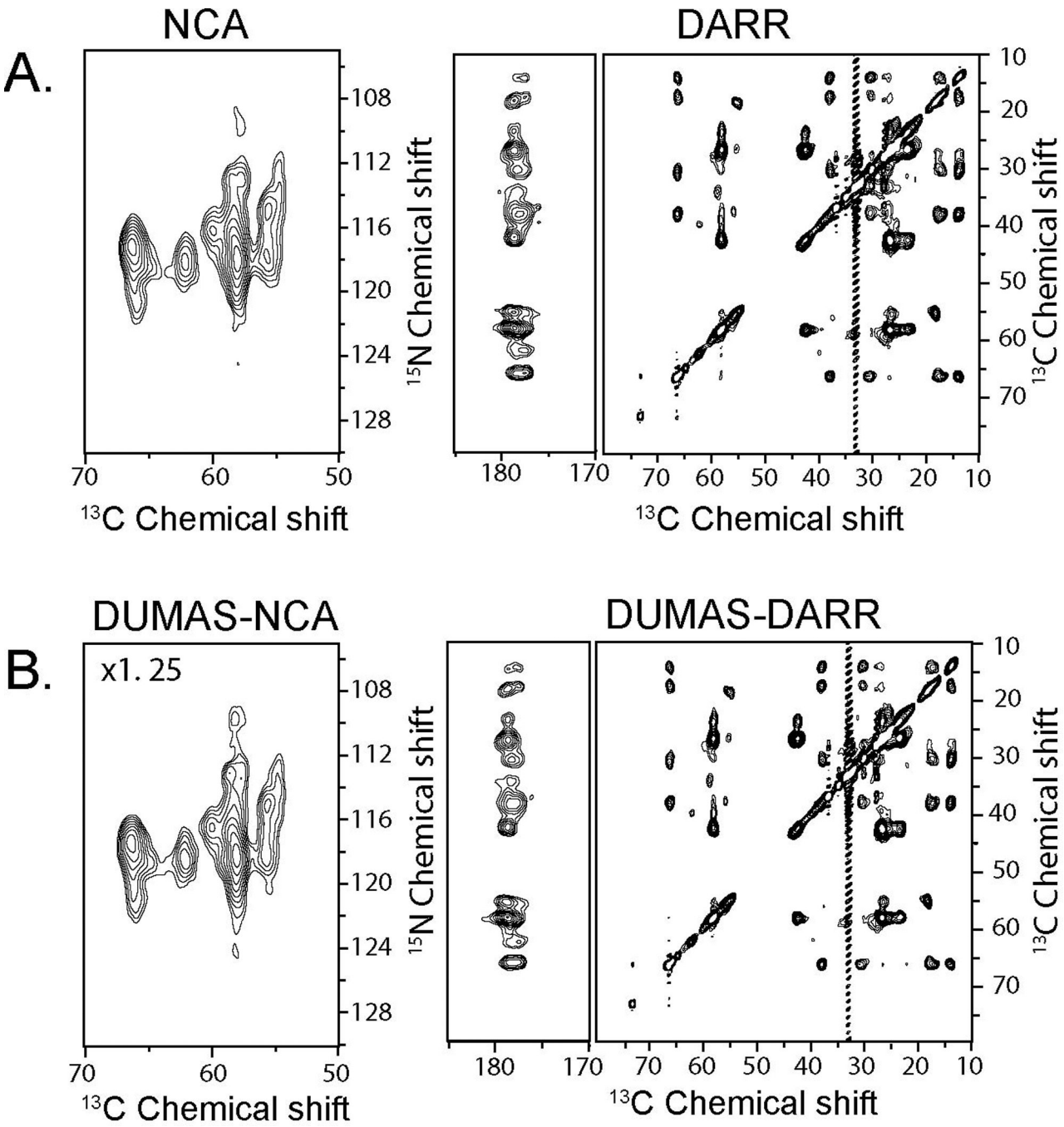

Figure 4.

(A) 2D NCA and DARR spectra of U-^{13}C,^{15}N-labeled phospholamban reconstituted in lipid membranes acquired using conventional methods (Figure 1S). (B) NCA and DARR spectra acquired simultaneously using DUMAS-DARR-NCA pulse scheme. As for the previous spectra, DARR and DUMAS-DARR are plotted with the identical noise level. DUMAS-NCA is plotted at 1.25 times the signal intensity of NCA to account for 20% signal loss of ^{15}N during SIM-CP.